J|A|C|S
ARTICLES
Published on Web 07/12/2002

DNA Mediated Charge Transport: Characterization of a DNA Radical Localized at an Artificial Nucleic Acid Base

Matthias Pascaly, Jae Yoo, and Jacqueline K. Barton*

Contribution from the Division of Chemistry and Chemical Engineering, California Institute of Technology, Pasadena, California 91125

Received February 13, 2002. Revised Manuscript Received May 24, 2002

Abstract: DNA assemblies containing 4-methylindole incorporated as an artificial base provide a chemically well-defined system in which to explore the oxidative charge transport process in DNA. Using this artificial base, we have combined transient absorption and EPR spectroscopies as well as biochemical methods to test experimentally current mechanisms for DNA charge transport. The 4-methylindole radical cation intermediate has been identified using both EPR and transient absorption spectroscopies in oxidative flash-quench studies using a dipyridophenazine complex of ruthenium as the intercalating oxidant. The 4-methylindole radical cation intermediate is particularly amenable to study given its strong absorptivity at 600 nm and EPR signal measured at 77 K with $g = 2.0065$. Both transient absorption and EPR spectroscopies show that the 4-methylindole is well incorporated in the duplex; the data also indicate no evidence of guanine radicals, given the low oxidation potential of 4-methylindole relative to the nucleic acid bases. Biochemical studies further support the irreversible oxidation of the indole moiety and allow the determination of yields of irreversible product formation. The construction of these assemblies containing 4-methylindole as an artificial base is also applied in examining long-range charge transport mediated by the DNA base pair stack as a function of intervening distance and sequence. The rate of formation of the indole radical cation is $\geq 10^7$ s^{-1} for different assemblies with the ruthenium positioned 17−37 Å away from the methylindole and with intervening A−T base pairs primarily composing the bridge. In these assemblies, methylindole radical formation at a distance is essentially coincident with quenching of the ruthenium excited state to form the Ru(III) oxidant; charge transport is not rate limiting over this distance regime. The measurements here of rates of radical cation formation establish that a model of G-hopping and AT-tunneling is not sufficient to account for DNA charge transport. Instead, these data are viewed mechanistically as charge transport through the DNA duplex primarily through hopping among well stacked domains of the helix defined by DNA sequence and dynamics.

Introduction

Charge transport through double helical DNA has been the subject of extensive studies owing to its relevance to our understanding of oxidative damage within the cell and its potential application in the development of DNA-based sensors.[1−6] With both goals as a focus, a mechanistic understanding of the charge transport process is essential.

Discrete, well-defined chemical assemblies containing either pendant donors and acceptors or nucleic acid base substitutions have been most useful in probing DNA charge transport.[1] The kinetics of DNA-mediated charge transport have been probed over a short distance regime (3−20 Å) using transient absorption and fluorescence spectroscopies.[7−12] DNA charge transport chemistry over longer distances has been primarily examined using biochemical methods, by analyzing the yield of the resultant DNA damage.[13−15] Through these studies, oxidative damage mediated by double helical DNA has been demonstrated over a distance of 200 Å.[16,17] Such damage depends sensitively upon the intervening DNA sequence and structure and can be

* To whom correspondence should be addressed. E-mail: jkbarton@caltech.edu.

(1) (a) Nunez, M. E.; Barton, J. K. *Curr. Opin. Chem. Biol.* **2000**, *4*, 199. (b) Kelly, S. O.; Barton, J. K. *Met. Ions Biol. Syst.* **1998**, *26*, 211.
(2) Schuster, G. B. *Acc. Chem. Res.* **2000**, *33*, 253.
(3) Giese, B. *Acc. Chem. Res.* **2000**, *33*, 631.
(4) Lewis, F. D.; Letsinger, R. L.; Wasielewski, M. R. *Acc. Chem. Res.* **2001**, *34*, 159.
(5) (a) Kelly, S. O.; Jackson, N. M.; Hill, M. G.; Barton, J. K. *Angew. Chem., Int. Ed.* **1999**, *38*, 941. (b) Boon, E. M.; Ceres, D. M.; Drummond, T. G.; Hill, M. G.; Barton, J. K. *Nat. Biotechnol.* **2000**, *18*, 1096. (c) Boon, E. M.; Barton, J. K. *Curr. Opin. Struct. Biol.* **2002**, *12*, 320.
(6) Murphy, C. J.; Arkin, M. R.; Jenkins, Y.; Ghatlia, N. D.; Bossman, S.; Turro, N. J.; Barton, J. K. *Science* **1993**, *262*, 1025.
(7) Kelley, S. O.; Barton, J. K. *Science* **1999**, *283*, 375.
(8) Lewis, F. D.; Wu, T.; Zhang, Y.; Letsinger, R. L.; Greenfield, S. R.; Wasielewski, M. R. *Science* **1997**, *277*, 673.
(9) Wan, C.; Fiebig, T.; Kelley, S. O.; Treadway, C. R.; Barton, J. K.; Zewail, A. H. *Proc. Natl. Acad. Sci. U.S.A.* **1999**, *96*, 6014.
(10) Wan, C.; Fiebig, T.; Schiemann, O.; Barton, J. K.; Zewail, A. H. *Proc. Natl. Acad. Sci. U.S.A.* **2000**, *97*, 14052.
(11) Hess, S.; Gotz, M.; Davis, W. B.; Michel-Beyerle, M. E. *J. Am. Chem. Soc.* **2001**, *123*, 10046.
(12) Kawai, K.; Takada, T.; Tojo, S.; Ichinose, N.; Majima. T. *J. Am. Chem. Soc.* **2001**, *123*, 12688.
(13) Hall, D. B.; Holmlin, R. E.; Barton, J. K. *Nature* **1996**, *382*, 731−735.
(14) (a) Meggers, E.; Kusch, D.; Spichty, M.; Wille, U.; Giese, B. *Angew. Chem., Int. Ed.* **1998**, *37*, 460−462. (b) Giese, B.; Wessely, S.; Spormann, M.; Lindemann, U.; Meggers, E.; Michel-Beyerle, M. E. *Angew Chem., Int. Ed.* **1999**, *38*, 996−998.
(15) Gasper, S. M.; Schuster, G. B. *J. Am. Chem. Soc.* **1997**, *119*, 12762.
(16) Nunez, M. E.; Hall, D. B.; Barton, J. K. *Chem. Biol.* **1999**, *6*, 85.
(17) Henderson, P. T.; Jones, D.; Hampikian, G.; Kan, Y.; Schuster, G. B. *Proc. Natl. Acad. Sci. U.S.A.* **1999**, *96*, 8353.

perturbed by DNA-binding proteins.[18−21] Mechanistically, on the basis of the spectroscopic studies at short range and biochemical studies at long range, a mixture of tunneling and hopping mechanisms have been proposed.[22−25]

In our laboratory, we have exploited primarily intercalators as pendant donors and acceptors; their stacking within the DNA helix offers an effective probe of the electronics of the π-stacked base pairs.[1] Metallointercalator−DNA conjugates have, moreover, proven to be particularly valuable. Complexes of Ru(II) containing the dipyridophenazine (dppz) ligand bind avidly to DNA by intercalation and provide sensitive luminescent probes of DNA.[26] Rhodium intercalators, structurally characterized bound to DNA,[27] serve as potent photooxidants and permit studies of long-range oxidative DNA damage on nucleosomes[28] and within the cell nucleus.[29]

Several kinetic experiments have been carried out over short distance regimes using artificial DNA bases. In particular, using 2-aminopurine as a fluorescent adenine analogue, base−base electron transfer has been probed.[7,9,10] Artificial bases can closely mimic the shape of the natural nucleosides and nucleotides. Furthermore, the steric as well as electrochemical properties of such molecules can be finely tuned by varying heteroatoms or substituents.[30] Such artificial bases are usually incorporated into the DNA for studying their cytotoxic behavior or influence on the structure of DNA.[31]

We have been interested in developing chemical assemblies that allow us to carry out both spectroscopic and biochemical measurements so as to follow the charge transport process through DNA and characterize radical intermediates. The flash-quench cycle with dppz complexes of ruthenium used to generate ruthenium(III) as the oxidant in situ has been extremely valuable in this effort.[32] The flash-quench technique was originally developed to explore charge transport reactions in proteins[33] but has been applied effectively in characterizing the neutral guanine radical in duplex DNA (Scheme 1). Excitation of the intercalated complex with visible light produces the corresponding excited-state complex *Ru(II), which can undergo electron transfer to the nonintercalating oxidative quencher $[Ru(NH_3)_6]^{3+}$. This yields the intercalated Ru(III) complex, a

Scheme 1. Schematic of the Flash-Quench Technique[a]

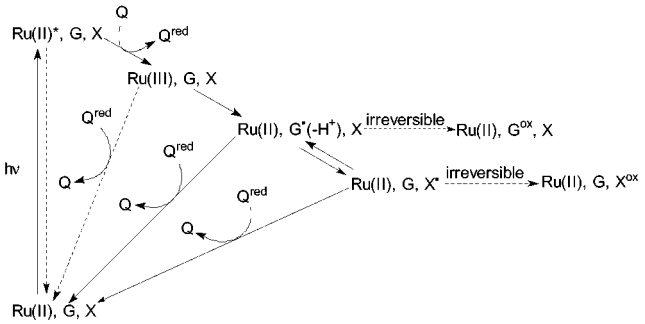

[a] Ru(II) = $[Ru(dppz)(phen)_2]^{2+}$ or $[Ru(bpy')(dppz)(phen)]^{2+}$, G = guanine, G^{ox} = oxidized guanine products, Q = quencher (e.g. $[Ru(NH_3)_6]^{3+}$, $[Co(NH_3)_5Cl]^{2+}$), Q^{red} = reduced state of Q, X = intercalated indole moiety (e.g. tryptophan, 4-methylindole), X^{ox} = oxidized indole products.

powerful ground state oxidant, that, based upon its electrochemical potential (1.5 V), can oxidize guanine. Guanine is the base with the lowest oxidation potential (1.3 V) among the naturally occurring nucleobases.[34,35] Given the low pK_A within the base pair with cytosine, only the neutral deprotonated guanine radical has been detected spectroscopically at times longer than 100 ns.[32]

Transient absorption spectroscopy and biochemical measurements of oxidative damage have been combined in characterizing protein radical intermediates generated by charge transport through DNA using the flash-quench technique.[36] The DNA-binding methylase M. *Hha*I is a base flipping enzyme that binds specifically to the sequence 5′-GCGC-3′ and inserts a glutamine side chain into the DNA, flipping out the internal cytosine base to facilitate its methylation.[37] We had observed that DNA charge transport to effect oxidative damage was inhibited upon binding of M. *Hha*I; disruption of the π-stack through base flipping shuts off the charge transport past the binding site of the enzyme.[20] Interestingly, we also observed that, in a mutant, in which the glutamine is mutated to a tryptophan, long-range oxidative damage is restored, consistent with the tryptophan side chain restoring the π-stack with the indole moiety. Furthermore, in mutant M. *Hha*I-bound DNA assemblies containing a pendant ruthenium intercalator, using the flash-quench method, we observed by transient absorption spectroscopy not only the guanine radical but also a signal corresponding to the neutral tryptophan radical.[36] In this system, the intercalated indole of the tryptophan has the lowest oxidation potential (1 V)[38] within the DNA stack and hence can be detected spectroscopically as an intermediate. The indole radical is easily identified owing to its significant absorptivity centered at 510 nm.[39] In comparison, the guanine radical absorbs more weakly with a small absorption feature centered at 390 nm. The guanine and tryptophan radicals undergo subsequent reactions with water

(18) Williams, T. T.; Odom, D. T.; Barton, J. K. *J. Am. Chem. Soc*. **2000**, *122*, 9048.
(19) Hall, D. B.; Barton, J. K. *J. Am. Chem. Soc*. **1997**, *119*, 5045.
(20) (a) Rajski, S. R.; Kumar, S.; Roberts, R. J.; Barton, J. K. *J. Am. Chem. Soc*. **1999**, *121*, 5615. (b) Rajski, S. R.; Barton, J. K. *Biochemistry* **2001**, *40*, 5556−5564.
(21) Bhattacharya, P. K.; Barton, J. K. *J. Am. Chem. Soc*. **2001**, *123*, 8649.
(22) (a)Giese, B.; Amaudrut, J.; Köhler, A.-K.; Spormann, M.; Wessely, S. *Nature* **2001**, *412*, 318−320. (b) Giese, B.; Spichty, M. *ChemPhysChem* **2000**, *1*, 195.
(23) (a) Meggers, E.; Michel-Beyerle, M. E.; Giese, B. *J. Am Chem. Soc*. **1998**, *120*, 12950. (b) Bixon, M.; Giese, B.; Wessely, S.; Lagenbacher, T.; Michel-Beyerle, M. E.; Jortner, J. *Proc. Natl. Acad. Sci. U.S.A.* **1999**, *96*, 11713.
(24) (a) Bixon, M.; Jortner, J. *J. Am. Chem. Soc*. **2001**, *123*, 12556. (b) Grozema, F. C.; Berlin, Y. A.; Siebbeles, L. D. A. *J. Am. Chem. Soc*. **2000**, *122*, 10903.
(25) Ly, D.; Sanii, L.; Schuster, G. B. *J. Am. Chem. Soc*. **1999**, *121*, 9400.
(26) Friedman, A. E.; Chambron, J.-C.; Sauvage, J.-P.; Turro, N. J.; Barton, J. K. *J. Am. Chem. Soc*. **1990**, *112*, 4960.
(27) Kielkopf, C. L.; Erkkila, K. E.; Hudson, B. P.; Barton, J. K.; Rees, D. C. *Nat. Struct. Biol*. **2000**, *7*, 117.
(28) Nunez, M. E.; Noyes, K. T.; Barton, J. K. *Chem. Biol*., in press.
(29) Nunez, M. E.; Holmquist, G. P.; Barton, J. K. *Biochemistry* **2001**, *40*, 12465.
(30) Kool, E. T.; Morales, J. C.; Guckian, K. M. *Angew. Chem., Int. Ed*. **2000**, *39*, 990.
(31) Moran, S.; Ren, R. X. F.; Sheils, C. J.; Rumney, S. IV; Kool, E. T.; *Nucleic Acids Res.* **1996**, *24*, 2044.
(32) Stemp, E. D. A.; Arkin, M. R.; Barton, J. K. *J. Am. Chem. Soc*. **1997**, *119*, 2921.
(33) Chang, I. J.; Gray, H. B.; Winkler, J. R. *J. Am. Chem. Soc*. **1991**, *113*, 7056.
(34) Steenken, S.; Jovanovic, S. V. *J. Am. Chem. Soc.* **1997**, *119*, 617.
(35) (a) Saito, I.; Takayama, M.; Sugiyama, H.; Nakatani, K.; Tsuchida, A.; Yamamoto, M. *J. Am. Chem. Soc.* **1995**, *117*, 6406. (b) Prat, F.; Houk, K. N.; Foote, C. S. *J. Am. Chem. Soc.* **1998**, *120*, 845.
(36) Wagenknecht, H. A.; Rajski, S. R.; Pascaly, M.; Stemp, E. D. A.; Barton, J. K. *J. Am. Chem. Soc.* **2001**, *123*, 4400.
(37) (a) Roberts, R. J.; Cheng, X.; *Annu. Rev. Biochem.* **1998**, *67*, 181. (b) Cheng, X.; Kumar, S.; Posfai, J.; Pflugrath, J. W.; Roberts, R. J. *Cell* **1993**, *74*, 299. (c) Klimasauskas, S.; Kumar, S.; Roberts, R. J.; Cheng, X. *Cell* **1994**, *76*, 357. (d) O'Gara, M.; Klimasauskas, S.; Roberts, R. J.; Cheng, X. *J. Mol. Biol.* **1996**, *261*, 634. (e) Mi, S.; Alonso, D.; Roberts, R. J. *Nucleic Acids Res.* **1995**, *23*, 620.
(38) DeFelippis, M. R.; Murphy, C. P.; Broitman, F.; Weinraub, D.; Faraggi, M.; Klapper, M. H. *J. Phys. Chem.* **1991**, *95*, 3416.
(39) Prütz, W. A.; Land, E. J. *Int. J. Radiat. Biol.* **1979**, *36*, 513.

and oxygen to form irreversible products which are used to visualize the location of DNA damage biochemically.[40] We had also carried out earlier experiments to characterize peptide radical intermediates utilizing tripeptides (Lys-Trp-Lys and Lys-Tyr-Lys) for probing the oxidation of the intercalated aromatic residue through DNA-mediated charge transport.[41]

Radical intermediates in DNA have also been explored using EPR spectroscopy.[42−44] These studies have focused on DNA radicals generated through either steady state ionizing radiation or pulse radiolysis or using noncovalently bound radical dopants. Without radicals generated at discrete positions within the chemical assemblies, perhaps not surprisingly, these studies have yielded conflicting results regarding DNA charge transport.

Here, we describe the characterization of a DNA assembly containing an artificial base, 4-methylindole, in which a radical intermediate within the base pair stack is generated using the flash-quench technique. This system serves as a model for peptide radicals intercalated within DNA. The methylindole radical, positioned at a discrete position within the helix, has been characterized by transient absorption and EPR spectroscopies, and the resultant irreversible damage has also been monitored biochemically. Using these chemical assemblies, following the formation of the radical intermediate, we have examined the distance dependence of charge transport through the DNA duplex. These assemblies provide a powerful system for mechanistically delineating long-range charge transport within the DNA π-stack.

Experimental Section

All chemical reagents and starting materials were purchased from commercial sources and used as received. The ligands bpy′ and dppz were synthesized according to literature procedures.[45−47] The syntheses of the complexes $[Ru(dppz)(phen)_2]Cl_2$ and $[Ru(bpy')(dppz)(phen)]Cl_2$ are described elsewhere.[46,47]

DNA Synthesis. The oligonucleotides were prepared on an Applied Biosystems 394 DNA synthesizer using standard phosphoramidite chemistry.[48] 5′-Dimethoxytrityl-2′-deoxy-4-methylindole-ribofuranosyl and 5′-dimethoxytrityl-2′-deoxyinosine phosphoramidites were purchased from Glen Research. After HPLC purification and lyophilization, the oligonucleotides were characterized with MALDI-TOF mass spectrometry. Single stranded DNA oligonucleotides were quantitated by their absorbance at 260 nm. Duplexes of the DNA oligonucleotides were formed with a 1:1 mixture of the complementary strands by heating to 90 °C for 5 min followed by slow cooling to ambient temperature over a time of 2 h in 10 mM Tris HCl, pH 8 for the transient absorption spectroscopy, in 10 mM NaP_i, 10 mM NaCl, pH 7 buffer for EPR spectroscopy, and in 25 mM NH_4OAc, pH 9 for the biochemical experiments.

For the synthesis of the ruthenated DNA oligonucleotides, a racemic mixture of the tris(heteroleptic) complex $[Ru(bpy')(dppz)(phen)]Cl_2$ was reacted with the oligonucleotide on a solid-phase support. Details of the reaction were taken from the literature.[49] Purification with C18 reverse-phase HPLC yields four isomers, which were characterized by UV−vis spectroscopy and MALDI-TOF mass spectrometry. Only one diastereomer was used for the laser spectroscopy and biochemical experiments, but the mixture of diastereomers was used for EPR measurements.

Laser Spectroscopy. After annealing the DNA assemblies in 10 mM TRIS, pH 8 buffer, the time-resolved emission and transient absorption experiments were carried out in the same buffer and utilized a YAG-OPO laser for excitation of the ruthenium lumiphore (λ_{ex} = 470 nm).[32] The emission of the intercalated ruthenium complexes was monitored at 610 nm. Emission intensities were obtained by integrating under the decay curve for the luminescence. The ruthenium luminescence was quenched with 20 equiv of $[Ru(NH_3)_6]Cl_3$, resulting in the loss of 85−95% of the emission. Noncovalently bound intercalators, when used, were added at a concentration of 30 μM after duplex annealings were complete. The transient absorption spectrum was generated by fitting the decay of the transient absorption traces from single wavelengths at times >5 μs to a monoexponential function ($y(t) = C_0 + C_1\exp(-k_1t)$) using $k_1 = 2 \times 10^5\ s^{-1}$ as the average rate constant. The absorbance changes were extrapolated to the zero-time absorbances calculated by the fit.

EPR Spectroscopy. EPR spectra were recorded using an X-band Bruker EMX spectrometer equipped with a standard TE_{102} cavity. Magnetic field calibrations were made against a degassed solution of 1% perylene in H_2SO_4. All measurements were made on photolyzed frozen samples at 77 K employing a finger dewar filled with liquid nitrogen designed to fit inside the EPR cavity. Photolysis was carried out by illuminating a 100 μL sample solution contained in quartz tubes (4 mm o.d.) while freezing in an optical dewar filled with liquid nitrogen. The light source used was a 300 W Xe-arc lamp (Varian Eimac Division, Light R300-3) powered by an Illuminator power supply (Varian Eimac Division, model PS 300-1). UV filters were employed to eliminate light <320 nm, and water was employed to eliminate IR radiation. The experiments were carried out with a duplex concentration of 25 μM in 10 mM sodium phosphate, 10 mM NaCl, pH 7. The solution contained 40 equiv of $[Co(NH_3)_5Cl]Cl_2$ as quencher.

Irradiation Experiments and Gel Electrophoresis. The oligonucleotides were labeled at the 5′-end using γ-^{32}P-ATP and polynucleotide kinase.[50] After desalting, the reaction mixture was purified on a 10% denaturing polyacrylamide gel. The desired band was cut from the gel, soaked in 1 mL of 500 mM NH_4OAc, and isolated by use of Micro Bio-Spin columns. Samples used in irradiations were annealed by cooling to 5 °C using 25 mM aq NH_4OAc, pH 9 as solvent. Irradiations (434 nm) were performed at 5 °C on 11 μL samples (c_{DNA} = 5 μM) using a 1000 W Hg/Xe-arc lamp equipped with a monochromator. In experiments where intercalator was bound noncovalently to the duplex, the concentration of the ruthenium intercalator was also 5 μM. $[Ru(NH_3)_6]^{3+}$ (20 equiv) was used as a quencher. After irradiation, the samples were treated with piperidine/water (1:9), heated to 90 °C for 25 min, and dried in vacuo. These samples were directly diluted into denaturing, gel loading buffer containing formamide. Sequencing gels were 20% denaturing polyacrylamide containing 8 M urea, and after electrophoresis, samples were analyzed by phosphorimagery.

Electrochemistry. Ground-state oxidation and reduction potentials for 4-methylindole were obtained on a Bioanalytical Systems (BAS) model CV-50W electrochemical analyzer. A glassy carbon working

(40) Burrows, C. J.; Muller, J. G.; *Chem. Rev.* **1998**, *98*, 1109.
(41) (a) Wagenknecht, H. A.; Stemp, E. D. A.; Barton, J. K. *J. Am. Chem. Soc.* **2000**, *122*, 1. (b) Wagenknecht, H. A.; Stemp, E. D. A.; Barton, J. K. *Biochemistry* **2000**, *39*, 5483.
(42) (a) Novais, H. M.; Steenken, S. *J. Am Chem. Soc.* **1986**, *108*, 1. (b) Graslund, A.; Ehrenberg, A.; Rupprecht, A.; Strom, G. *Biochim. Biophys. Acta* **1971**, *254*, 172. (c) Barnes, J.; Bernhard, W. A. *J. Phys. Chem.* **1993**, *97*, 3401.
(43) (a) Pezeshk, A.; Symons, M. C. R.; McClymont, J. D. *J. Phys. Chem.* **1996**, *100*, 18562. (b) Cullis, P. M.; McClymont, J. D.; Symons, M. C. R. *J. Chem. Soc., Faraday Trans.* **1990**, *86*, 591.
(44) Schiemann, O.; Turro, N. J.; Barton, J. K. *J. Phys. Chem. B.* **2000**, *104*, 7214.
(45) Della Ciena, L.; Hamachi, I.; Meyer, T. J. *J. Org. Chem.* **1989**, *54*, 1731.
(46) Dupureur, C. M.; Barton, J. K. *Inorg. Chem.* **1997**, *36*, 33.
(47) (a) Amouyal, E.; Homsi, A.; Chambron, J.-C.; Sauvage, J.-P. *J. Chem. Soc., Dalton Trans.* **1990**, 1841. (b) Strouse, G. F.; Anderson, P. A.; Schoonover, J. R.; Meyer, T. J.; Keene, F. R. *Inorg. Chem.* **1992**, *31*, 3004. (c) Anderson, P. A.; Deacon, G. B.; Haarman, K. H.; Keene, F. R.; Meyer, T. J.; Reitsma, D. A.; Skelton, B. W.; Strouse, G. F.; Thomas, N. C.; Treadway, J. A. *Inorg. Chem.* **1995**, *34*, 6145.
(48) (a) Beaucage, S. L.; Caruthers, M. H. *Tetrahedron Lett.* **1981**, *22*, 1859. (b) Goodchild, J. *Bioconjugate Chem.* **1990**, *1*, 165.
(49) Holmlin, R. E.; Dandliker, P. J.; Barton, J. K. *Bioconjugate Chem.* **1999**, *10*, 1122.
(50) Sambrook, J.; Fritsch, E. F.; Maniatis, T. *Molecular Cloning: A Laboratory Manual*, 2nd ed.; Cold Spring Harbor Laboratory: New York, 1989.

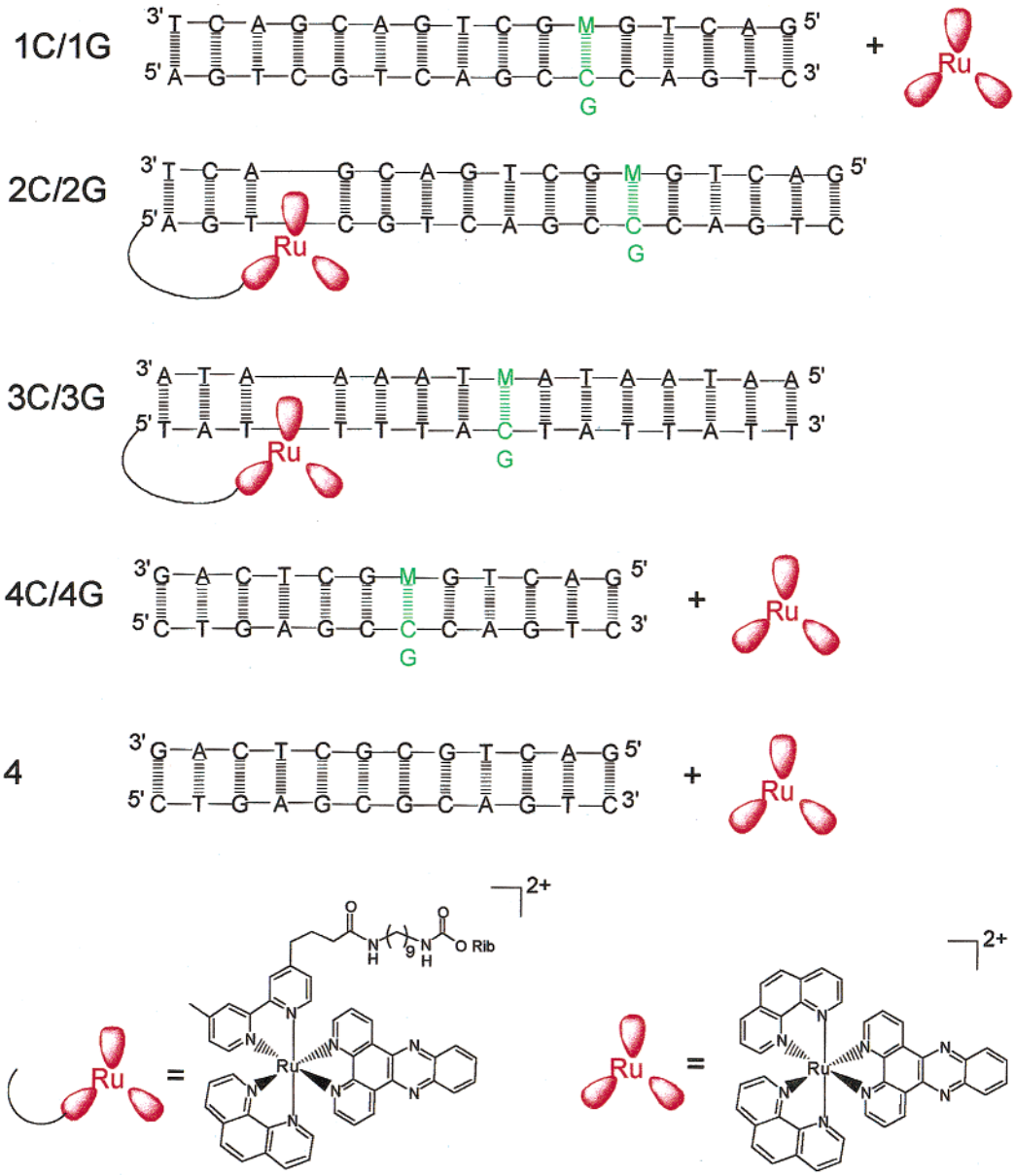

Figure 1. DNA substrates **1**−**4** and the structures of the ruthenium(II) complexes used in this study. C and G denote the bases used as a complementary base for the methylindole nucleoside.

electrode, Ag/AgCl reference electrode, and Pt auxiliary electrode were used in a single cell sample apparatus. A solution of 4-methylindole (1 mM) in dry acetonitrile (Fluka; stored over molecular sieves) containing 100 mM tetrabutylammonium hexafluorophosphate was degassed with Ar prior to use, and the voltammogram was collected using a 100 mV/s scan rate. The oxidation potential is reported in volts versus NHE.

Results and Discussion

Synthetic Design of DNA Assemblies. The DNA assemblies we prepared include a 4-methylindole nucleoside at a discrete position within the duplex. The 4-methylindole was embedded between two G bases in the sequence 5′-GMGC-3′ analogously to our earlier study of an intercalated tryptophan of the M. *Hha*I mutant bound to a ruthenated DNA (Figure 1).[36] The incorporation of 4-methylindole into the DNA is known to destabilize the duplex.[30,51] Although 4-methylindole exhibits reasonable stacking ability within the DNA, the artificial base pairs very poorly with natural Watson−Crick bases in duplex DNA.[52] A structurally similar artificial base (4-methylbenzimidazole) is nonselective in its base pairing, destabilizing the DNA by roughly the same amount when paired with any of the four natural bases. Accordingly, both guanine and cytosine were examined as complementary bases for 4-methylindole. Compared to normal Watson−Crick DNA, these oligonucleotides exhibit a decreased melting temperature and a shallow melting curve which reflects the effect of the 4-methylindole. For the EPR studies, 4-methylindole was included within an AT-containing oligomer lacking any guanines. This is essential for the EPR experiments, because the signal of a guanine radical would dominate the spectrum.[44] For control purposes, an

(51) (a) Guckian, K. M.; Morales, J. C.; Kool, E. T. *J. Org. Chem.* **1998**, *63*, 9652. (b) Kool, E. T. *Annu. Rev. Biophys. Biomol. Struct.* **2001**, *30*, 1.
(52) (a) Guckian, K. M.; Schweitzer, B. A.; Ren, R. X.-F.; Sheils, C. J.; Paris, P. L.; Tahmassebi, D. C.; Kool, E. T. *J. Am. Chem. Soc.* **1996**, *118*, 8182. (b) Loakes, D.; Hill, F.; Brown, D. M.; Salisbury, S. A. *J. Mol. Biol.* **1997**, *270*, 426.

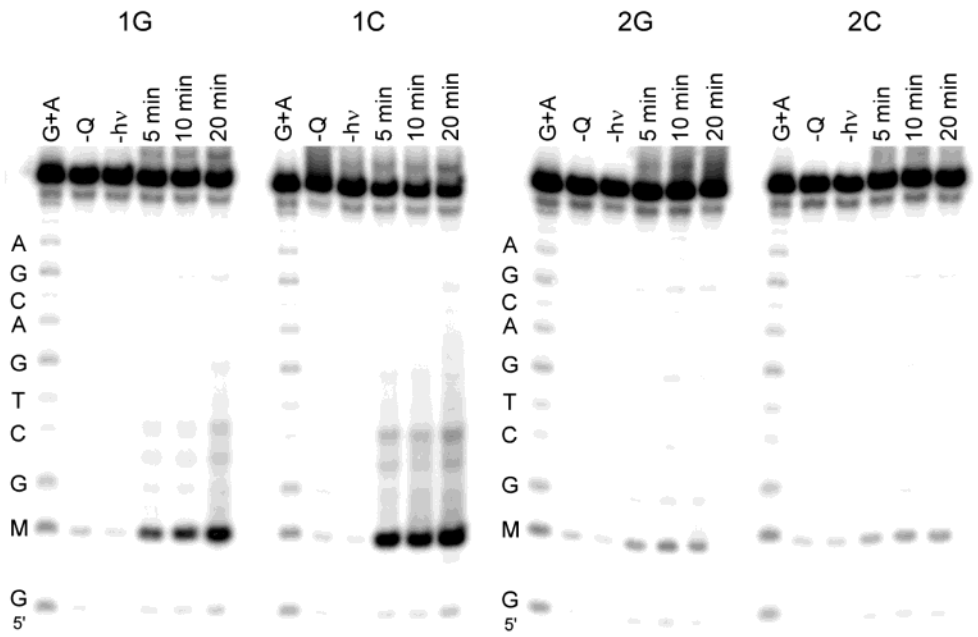

Figure 2. Phosphorimagery following gel electrophoretic analysis of oligonucleotides **1** (left) and **2** (right) after irradiation and treatment with piperidine. For sequence **1**, samples contained DNA (5 μM), $[Ru(dppz)(phen)_2]^{2+}$ (5 μM), and $[Ru(NH_3)_6]^{3+}$ (100 μM) in 25 mM aq NH_4OAc at pH 9; $\lambda_{ex} = 470$ nm. Using the Ru−DNA conjugate, samples contained **2** (5 μM) and $[Ru(NH_3)_6]^{3+}$ (100 μM) in 25 mM aq NH_4OAc at pH 9; $\lambda_{ex} = 470$ nm. Samples were irradiated with a HeCd laser at $\lambda_{ex} = 442$ nm for 5, 10, or 20 min. The control samples contained all the listed components, but light ($-h\nu$) or quencher ($-$Q) was excluded. After irradiation, samples were treated with 10% piperidine at 90 °C for 25 min and analyzed on a denaturing polyacrylamide (20%) DNA sequencing gel.

analogous DNA duplex lacking 4-methylindole was also synthesized, where the 4-methylindole was substituted with cytosine.

The oxidation potential of 4-methylindole in acetonitrile was found to be approximately 1.0 V versus NHE, similar to other methylindoles and tryptophans. How the environment within the duplex may perturb this value is not known. Nonetheless, we expect that, within these assemblies, 4-methylindole is the site of lowest oxidation potential.

Ruthenium intercalators were employed as oxidants in these experiments. $[Ru(bpy')(dppz)(phen)]^{2+}$ was tethered to the 5′ end of oligomers; earlier work established that this tethered complex intercalates 2−3 base pairs from the end of the duplex.[53] Some experiments were carried out using noncovalently bound $[Ru(dppz)(phen)_2]^{2+}$, which intercalates nonspecifically at sites across the duplex.

The incorporation of 4-methylindole into these DNA assemblies provides several advantages over earlier systems with bound peptide or protein.[36,41] Most importantly, with the indole moiety incorporated as an artificial base, the exact location is now unambiguous. Additionally, the elimination of the enzyme allows for the experiments to be carried out at different salt concentrations and temperatures. Moreover, the oxidative quenching is more efficient when there is no peptide or protein to compete with the quencher for binding sites on the DNA.

Biochemical Analysis of 4-Methylindole Oxidation in DNA Duplexes using the Flash-Quench Method. We examined oxidative damage within the DNA assembly using both noncovalently and covalently bound ruthenium intercalator. A 16 base pair DNA duplex was used for photoirradiation experiments. After irradiation at 434 nm in the presence of 20 equiv of $[Ru(NH_3)_6]Cl_3$, oxidative damage to the DNA can be visualized by treatment with piperidine and subsequent analysis by 20% denaturing PAGE. The experiments show that damage to the DNA occurs preferentially at the 4-methylindole site (Figure 2) and that the formation of this damage requires both light and quencher. With the untethered $[Ru(dppz)(phen)_2]^{2+}$, bound indiscriminately on the DNA, extensive damage at the 4-methylindole site is evident. With $[Ru(bpy')(dppz)(phen)]^{2+}$ covalently tethered near the duplex terminus and 4-methylindole located 8 base pairs away from the Ru intercalation site, long-range charge transport leads also to oxidative damage exclusively at the artificial base (Figure 2).

As observed in earlier studies, the efficiency of oxidation is higher with noncovalent oxidant.[13,53] This higher efficiency is consistent with more effective stacking and the longer excited state lifetime of the noncovalent intercalator. In the assemblies containing 4-methylindole, the difference in efficiency for oxidation with covalent versus noncovalently bound ruthenium may be further enhanced owing to specific binding of noncovalent ruthenium at the 4-methylindole site. Such binding may serve to stabilize the artificial base within the helix; variations in efficiency as a function of distance separating the intercalator from the 4-methlindole are small (vide infra) and cannot account for the differences seen.

Assemblies with guanine or cytosine as complementary base for 4-methylindole were also examined. The results clearly show that the extent of damage of the artificial base does not depend on its complementary base. With both guanine and cytosine, approximately the same amount of oxidative damage of the 4-methylindole has been observed.

Attempts were made to further characterize the damage at the 4-methylindole position using HPLC analysis after enzymatic digestion.[41] These experiments were not successful,

(53) Arkin, M. R.; Stemp, E. D. A.; Coates Pulver, S.; Barton, J. K. *Chem. Biol.* **1997**, *4*, 389.

however. Only one 4-methylindole could be incorporated within an oligomer to maintain duplex stability, a key requirement for long-range oxidative damage, but this limited the quantity of material being examined. The HPLC experiments, however, revealed no appreciable damage above that seen by gel electrophoresis after piperidine treatment.

In these experiments, no significant damage is observed at guanines on the strand that contains the 4-methylindole. In earlier studies with intercalated tryptophan, oxidative damage at the guanine positioned on the 5′-side of the indole was evident, and transient absorption experiments revealed a mixture of both tryptophan and guanine radicals.[36] We proposed in those cases that stacking of the tryptophan might lower the oxidation potential of the 5′-G as with the 5′-G within guanine doublets. Here, however, the stacking orientation differs. Certainly, access for trapping of the guanine radical to yield oxidative products would be expected to be greater in the present assemblies compared to those with bound peptide or protein. In any case, it is apparent that in these assemblies the oxidation potential of the indole moiety must be sufficiently low compared to that of the neighboring guanine so that no appreciable radical density resides on the guanine site.

These experiments show that 4-methylindole is well incorporated into the DNA π-stack despite the fact that it cannot form hydrogen bonds with its complementary base. Damage from a distance through long-range charge transport does occur to promote oxidative lesions centered at the 4-methylindole site.

EPR Spectroscopy on DNA Assemblies Containing 4-Methylindole. An organic radical within the DNA duplex containing 4-methylindole, once generated by the flash-quench method, can be monitored directly using EPR spectroscopy. EPR measurements were made on a 15 mer duplex covalently modified at one end with a ruthenium complex (Figure 1, sequence **3**). The sequence of this duplex contains only ATs with a single 4-methylindole moiety located approximately 17 Å (5 base pairs) from the site of intercalation of the ruthenium complex. The choice of this sequence without guanines avoids any complications in assignment associated with oxidation of guanines concomitantly to 4-methylindole; guanine radicals would produce overlapping signals.[44]

Figure 3 shows the EPR spectrum recorded at 77 K after flash-quench oxidation of assembly **3C** using $[Co(NH_3)_5Cl]Cl_2$ as the oxidative quencher. The cobalt complex was used as a quencher to enhance the lifetime of the radical, because this quencher in its reduced form aquates and back electron transfer is precluded.[32,53] As can be seen, a broad signal with no resolvable hyperfine features is observed. This signal has a g value of 2.0065 with a peak to trough width of 20 and 60 G in total width. Quencher, ruthenium, and light are all required to produce this radical signal. We also examined spectra from higher concentration solutions using noncovalently bound ruthenium as oxidant. In those instances, as well, no hyperfine features could be resolved. The radical is apparently stable only in frozen solutions; warming the solution to ambient temperatures and refreezing results in a total loss of signal. Also shown in Figure 3 is the control taken on an oligomer (AT) lacking the 4-methylindole; here, no distinct signal is evident. Hence, we can assign the signal to the 4-methylindole radical cation. The shape and overall width are consistent with those observed with tryptophan radical in a frozen medium.[54]

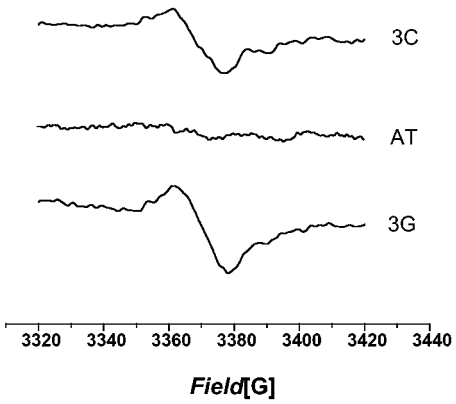

Figure 3. EPR spectra of Ru−DNA conjugates **3C** and **3G** recorded at 77 K upon flash-quench oxidation. The top trace is the spectrum of a duplex containing guanine opposite 4-methylindole (**3G**), the middle is that of an AT rich oligo, and the bottom is that of a duplex with a cytosine opposite the 4-methylindole (**3C**). Samples for the EPR measurement contain 25 μM Ru−DNA conjugate and 800 μM $[Co(NH_3)_5Cl]^{2+}$ in 10 mM potassium phosphate, pH 7, 50 mM NaCl. Spectrometer settings: ν = 9.84 GHz, modulation frequency = 100 kHz, modulation amplitude = 10 G, microwave power = 6.36 mW, time constant = 0.64 ms, conversion time = 5.12 ms, 100 scans.

Table 1. Kinetic data for $[Ru(dppz)(phen)_2]^{2+}$ and the 4-Methylindole Radical (M_{rad})[a]

	sequence **4C** (M–C pair)	sequence **4G** (M–G pair)
luminescence lifetime of *$[Ru(dppz)(phen)_2]^{2+}$ [b]	τ_1 = 55 ns (72%); τ_2 = 265 ns (28%)	τ_1 = 40 ns (51%); τ_2 = 232 ns (39%)
decay of M_{rad}[c,d]	1.5×10^5 s^{-1}	1.5×10^5 s^{-1}
formation of M_{rad}[c,e]	2×10^6 s^{-1}	1×10^6 s^{-1}

[a] All samples contained 30 μM DNA, 30 μM $[Ru(dppz)(phen)_2]^{2+}$, 5 mM Tris HCl, pH 8. [b] The luminescence traces were fit to a biexponential function ($y(t) = 100[C_1 \exp(-t/\tau_1) + (1 - C_1)\exp(-t/\tau_2)]$) by nonlinear least-squares method with convolution of the instrument response function. Uncertainties in values are ±10%. [c] Sample contained 20 equiv of $[Ru(NH_3)_6]^{3+}$ as quencher. [d] The transient absorption decay at 600 nm corresponding to the 4-methylindole radical was fit to a monoexponential function by nonlinear least-squares methods. Uncertainties in values are ±10%. [e] The rise of the signal at 600 nm was fit to a monoexponential function by nonlinear least-squares method; with the bandwidth used and region fit, these values represent lower limits.

Also shown in Figure 3 is the EPR spectrum for sequence **3G**, in which a G is positioned opposite the 4-methylindole. The spectrum is identical to that where a C is the opposing base. We expect that a guanine radical is not contributing to this signal, given, first, that the spectrum is identical to that of **3C** and, second, that the biochemical experiments (vide supra) provide no indication of the formation of a guanine radical in assemblies containing 4-methylindole as an artificial base.

Emission and Transient Absorption Studies on DNA Assemblies Containing 4-Methylindole. A 12 base pair oligonucleotide duplex (sequence **4C** and **4G**) and untethered $[Ru(dppz)(phen)_2]^{2+}$ (ratio 1:1) were used for luminescence investigations. Time-resolved luminescence measurements at 610 nm upon excitation at 470 nm indicate that the excited-state Ru complex, $*[Ru(dppz)(phen)_2]^{2+}$, decays biexponentially with τ_1 = 55 ns and τ_2 = 265 ns for the 4-methylindole-cytosine pair (Table 1). With guanine as complementary base opposing the 4-methylindole, similar values, τ_1 = 40 ns and τ_2 = 232 ns,

(54) (a) Moan, J.; Kaalhus, O. *J. Chem. Phys.* **1974**, *61*, 3556. (b) Dibilio, A, J.; Crane, B. R.; Wehbi, W. A.; Kiser, C. N.; Abu-Omar, M. M.; Carlos, R. M.; Richards, J. H.; Winkler, J. R.; Gray, H. B. *J. Am. Chem. Soc.* **2001**, *123*, 3181.

are observed. These values also resemble those reported earlier for dppz complexes of Ru(II) bound to DNA.[55] Therefore, significant quenching of the ruthenium(II) excited state by 4-methylindole does not occur. Addition of 10 equiv of $[Ru(NH_3)_6]^{3+}$ quenches the luminescence by 85% to 95%, permitting further experiments utilizing the flash-quench method.

Transient absorption spectroscopy was used to monitor the intermediates formed upon oxidative quenching of *[Ru(dppz)-$(phen)_2]^{2+}$ with $[Ru(NH_3)_6]^{3+}$. To identify the aromatic radical generated via the flash-quench experiments, absorbance difference spectra for the long-lived positive transient signals were obtained. With DNA substrate **4C**, the generated spectrum (Figure 4a) shows a characteristically sharp and intense positive absorbance at 340 nm as well as a broad absorbance of lower intensity centered at 550−650 nm. A broad negative absorbance is apparent at 440 nm.

As a reference, we also synthesized a DNA substrate in which 4-methylindole was replaced by cytosine. Employing the flash-quench technique with $[Ru(dppz)(phen)_2]^{2+}$ on this duplex yields a spectrum that is dominated by the broad and intense negative absorbance at 440 nm (Figure 4a), owing to the loss of the metal-to-ligand charge-transfer (MLCT) band that is characteristic for ruthenium polypyridyl complexes.[32,56] This spectrum in particular lacks the broad positive absorbance between 550 and 650 nm seen for assembly **4C**. However, the spectrum also exhibits a positive absorbance feature at 340 nm. With these features, the observed spectrum can be assigned solely to the $Ru^{3+}-Ru^{2+}$ absorbance difference for the dppz complex.[56]

After normalization, subtraction of the ruthenium difference spectrum from the transient absorption spectrum of sequence **4C** yields a spectrum with absorbances at 340 nm and 550−650 nm (Figure 4b). The recorded spectrum corresponds closely to the spectrum of the 4-methylindole radical cation obtained using pulse radiolysis experiments,[57] where characteristic bands at 335 and 560 nm were observed. Hence, we assign this resultant spectrum to that of the 4-methylindole radical cation formed in the DNA assembly. Such a shift of UV−vis absorption bands to longer wavelengths is commonly observed upon intercalation.[41,58] The bathochromic shift observed in the transient absorption spectrum of the 4-methylindole radical cation therefore suggests that this artificial base is well incorporated into the DNA π-stack. The absorbance signal between 550 and 650 nm can be used to discern the kinetic behavior of the generated 4-methylindole radical cation.

Under our experimental conditions, two species are detected in solution, which results in the mixture of positive and negative absorbance signals: the 4-methylindole radical cation contributes to the two positive signals, while the strongly negative signal in the 400−500 nm region is derived from the remaining unreacted Ru(III).

Figure 5 shows the formation and decay of the transient absorption signal at 600 nm generated with sequence **4C** and $[Ru(dppz)(phen)_2]^{2+}$. The short-lived transient at 600 nm corresponds to the generated 4-methylindole radical, where an

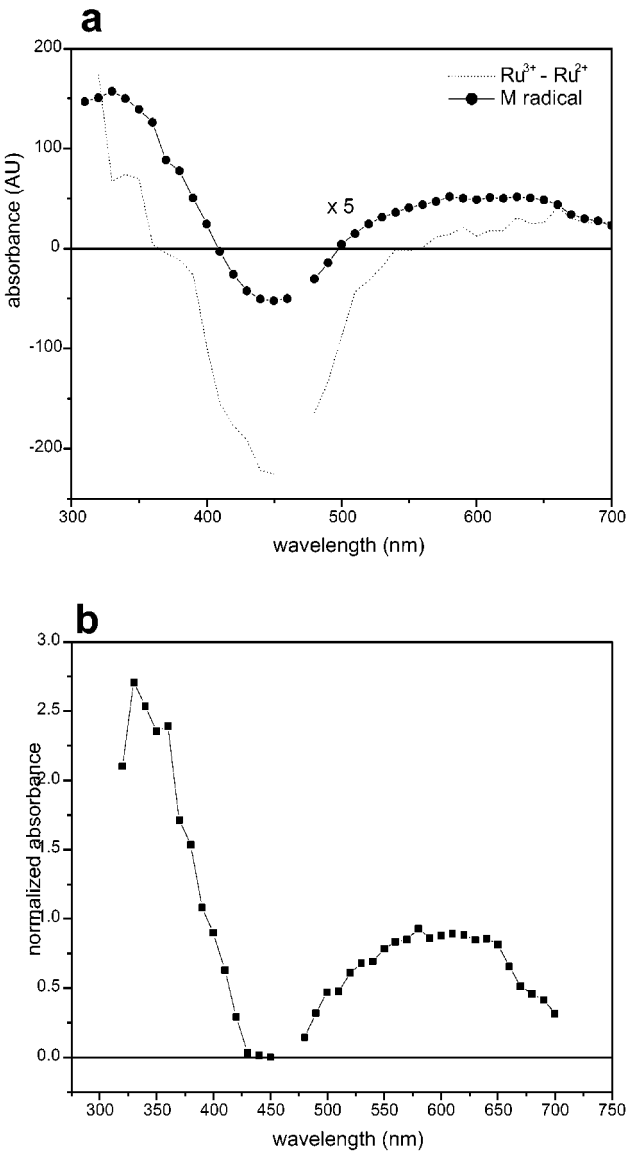

Figure 4. (a) Absorbance difference spectrum observed for **4C** obtained through the flash-quench technique (−•−). Also shown is the $Ru^{3+}-Ru^{2+}$ difference spectrum for $[Ru(dppz)(phen)_2]^{2+}$ obtained with **4** (···). The decay of the transient absorbances of individual signals was fit to the mono-exponential function $A(t) = C + A(t = 0)[\exp(-kt)]$ with $k = 2 \times 10^5\ s^{-1}$. $A(t = 0)$ was plotted against the wavelength. The sample contained **4C** (30 μM), $[Ru(dppz)(phen)_2]^{2+}$ (30 μM), and $[Ru(NH_3)_6]^{3+}$ (600 μM) in 5 mM TRIS buffer at pH 8; $\lambda_{ex} = 470$ nm. (b) Absorbance difference spectrum obtained after subtraction of the ruthenium difference spectrum from the spectrum obtained with 4-methylindole containing DNA **4C**. Prior to the calculation, both spectra were normalized to the most negative absorbance (at 450 nm).

absorbance maximum is observed. The signal at 600 nm initially is negative, owing to residual $*[Ru(dppz)(phen)_2]^{2+}$ emission, but the signal crosses over the baseline to give a positive signal, corresponding to the formation of the 4-methylindole radical. This radical forms on a time scale of <5 μs (Table 1). This time scale for radical formation is similar to that seen in earlier experiments with the DNA-binding protein.[36] The initial negative spike at short times can be attributed to emission from the dppz complex, because neither the hexaammine quencher nor the intercalator absorbs at 600 nm.

The signal of the 4-methylindole radical cation decays with a rate constant of $1.5 \times 10^5\ s^{-1}$. This decay of the 4-methyl-

(55) (a) Delaney, S.; Pascaly, M.; Bhattacharya, P.; Han, K.; Barton, J. K. *Inorg. Chem.* **2002**, *41*, 1966. (b) Lincoln, P.; Broo, A.; Norden, B. *J. Am. Chem. Soc.* **1996**, *118*, 2644.
(56) Stemp, E. D. A.; Barton, J. K. *Inorg. Chem.* **2000**, *39*, 3868.
(57) Solar, S.; Getoff, N.; Surdar, P. S.; Armstrong, D. A.; Gingh, A. *J. Phys. Chem.* **1991**, *95*, 3639−3643.
(58) Li, H.; Fedorova, O. S.; Grachev, A. N.; Trumble, W. R.; Bohach, G. A.; Czuchajowski, L. *Biochim. Biophys. Acta* **1997**, *1354*, 252−260.

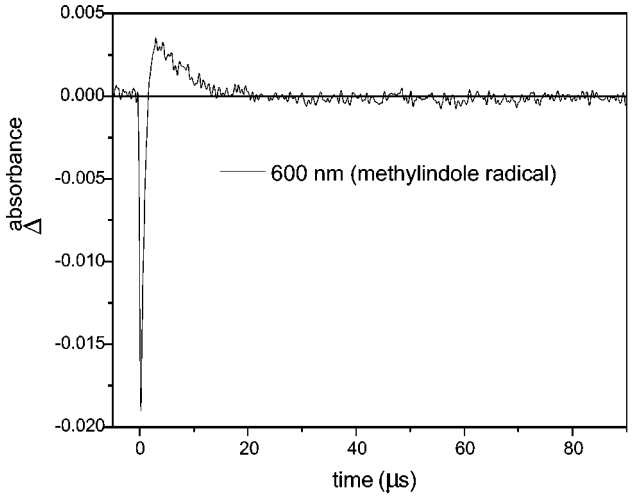

Figure 5. Time-resolved transient absorption traces at 600 nm (—) for the sample containing oligonucleotide **4C**. The sample consisted of **4C** (30 μM), $[Ru(dppz)(phen)_2]^{2+}$ (30 μM), and $[Ru(NH_3)_6]^{3+}$ (600 μM) in 5 mM TRIS buffer, pH = 8; λ_{ex} = 470 nm.

indole radical cation occurs an order of magnitude faster than in earlier experiments with a DNA binding protein which inserts a tryptophan side chain into the DNA.[36] This may reflect the higher solvent accessibility of the indole radical in these chemical assemblies compared to the DNA−protein complexes. Additionally, 4-methylindole does not bear any acidic protons, and thus, the radical cation is not depleted by proton transfer. The deprotonation of the radical cation would have a stabilizing effect, yielding an uncharged radical which is longer lived and therefore more susceptible for subsequent reactions with dioxygen or water.

Pairing 4-methylindole with cytosine or guanine influences the spectra of the generated radicals. Both spectra were obtained with $[Ru(dppz)(phen)_2]^{2+}$ which is noncovalently bound to the DNA duplex. The signals decay with the same rate constant of $k = 1.5 \times 10^5\ s^{-1}$. The transient absorption spectrum of duplex **4G** with a M−G base pair differs slightly in intensity (data not shown). The overall intensity is lower, and the absorption features are less well pronounced. This is a result of a lower yield of the generated transient 4-methylindole radical cation. We attribute this lower yield to the fact that in this duplex 4-methylindole is less well incorporated into the DNA π-stack. Guanine is a sterically more demanding base pairing partner and has therefore a more disruptive effect on the 4-methylindole stacking than does the smaller pyrimidine base cytosine. However, the lifetime of the 4-methylindole radical spectrum measured for duplexes **4C** and **4G** at 600 nm does not differ significantly (Table 1).

Distance Dependence of Charge Transport through Methylindole-Containing DNA. The incorporation of 4-methylindole

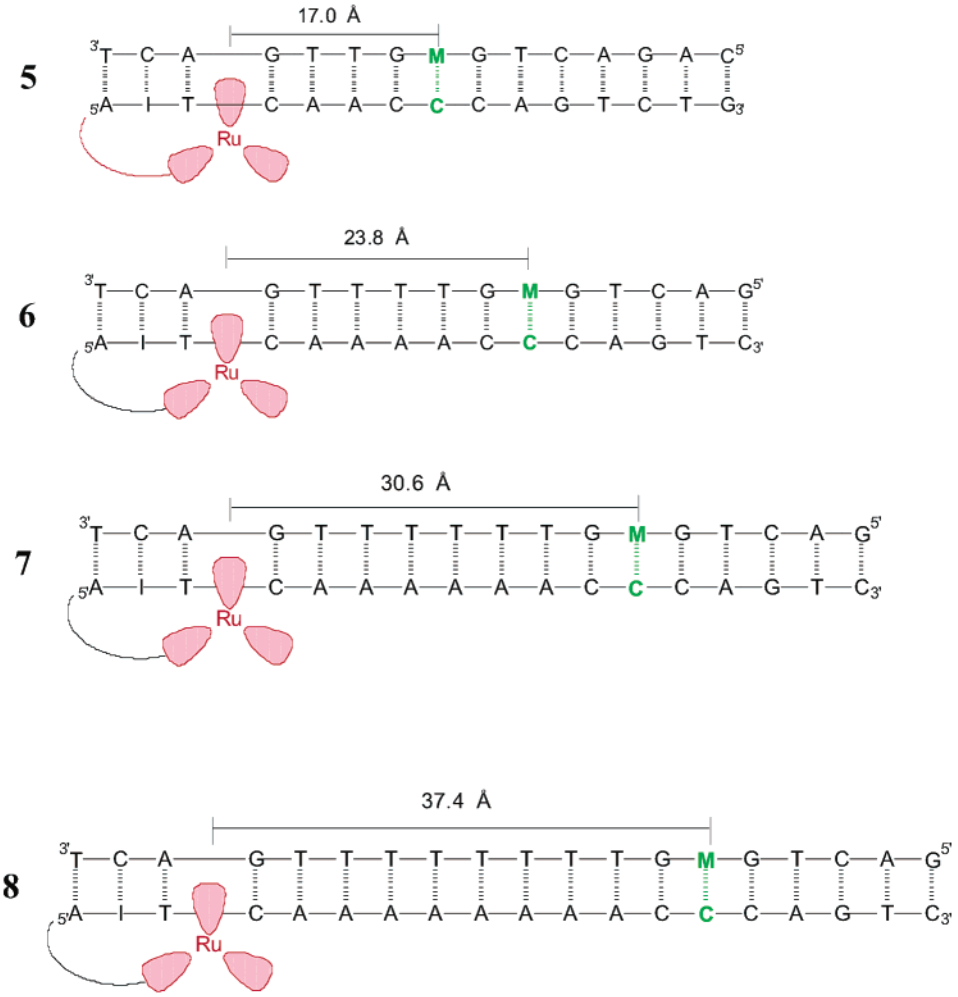

Figure 6. Schematic illustration of the DNA assemblies functionalized with the tethered photooxidant $[Ru(bpy')(dppz)(phen)]^{2+}$ used in this study. M = 4-methylindole nucleoside, I = inosine nucleoside.

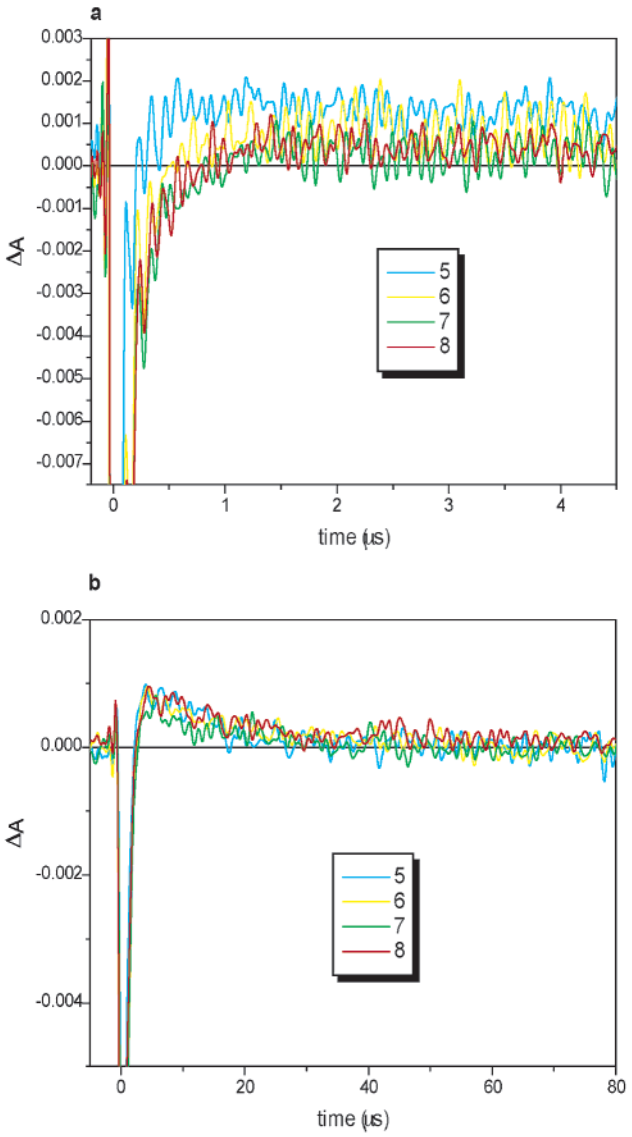

Figure 7. Time-resolved transient absorption traces at 600 nm. Shown are the results from sequences **5**−**8**. Sequence designations are shown in Figure 6. (a) Traces recorded over 5 μs. (b) Traces recorded over 100 μs. For both traces, the samples consisted of Ru−DNA (20 μM) and $[Ru(NH_3)_6]^{3+}$ (200 μM) in 5 mM TRIS buffer, pH = 8; λ_{ex} = 470 nm.

as an artificial base permits the systematic evaluation of DNA charge transport as a function of distance in these assemblies. Figure 6 shows the DNA sequences used to examine the distance dependence of charge transport. The lengths of the duplexes varied from 15 to 19 base pairs. As the photooxidant, $[Ru(bpy')(dppz)(phen)]^{2+}$ is tethered to the 5′ end of 1 oligonucleotide single strand. In the complementary strand, 4-methylindole is embedded between 2 guanine nucleosides. Earlier studies have shown that the ruthenium complex intercalates between the 3rd and the 4th base pair.[53] Hence, the length of the DNA bridge between the ruthenium intercalation site and the position of the 4-methylindole was varied from 17 Å, with two intervening Ts in **5**, to 37 Å, with 8 intervening Ts in **8**, assuming 3.4 Å stacking distances. We also included a single guanine base on the proximal side of the bridge close to the bound ruthenium. Because this is the base closest to the Ru-complex intercalation site with the lowest oxidation potential, one might anticipate that hole injection into the DNA bridge would occur preferentially at this base. The guanine on the Ru-complex bearing DNA strand was also replaced by inosine (I) to ensure hole injection only to the proximal guanine. Importantly, the bridge contained exclusively adenine and thymine bases, with thymine bases of variable number on the strand containing the 4-methylindole.

Table 2. Rates of Formation of the 4-Methylindole Radical Cation in Ru−DNA Sequences **5**−**8**

assembly[a]	G···G distance[b]	no. intervening thymines in bridge	rate constant[c]
5	13.6 Å	2	3.5×10^7 s^{-1}
6	20.4 Å	4	3.0×10^7 s^{-1}
7	27.2 Å	6	2.9×10^7 s^{-1}
8	34.0 Å	8	2.7×10^7 s^{-1}

[a] All samples contained 20 μM Ru-DNA, 200 μM $[Ru(NH_3)_6]^{3+}$, and 5 mM Tris HCl, pH 8, with λ_{exc}= 470 nm. Power of the YAG-OPO laser ranged from 3 to 3.5 mJ/pulse. [b] The distance here corresponds to that between the proximal single guanine base and the 3′-G of the 3′-GMG-5′ triplet assuming 3.4 Å base−base stacking. [c] For formation of 4-methylindole radical cation (600 nm). The transient absorption traces at 600 nm correspond to absorptivity of the 4-methylindole radical and were fit to a monoexponential function by nonlinear least-squares methods. These values, close to the instrument response and emission decay rate, represent lower limits in the rate of radical formation. At 440 nm, reflecting charge injection, the Ru^{3+}−Ru^{2+} recovery rate was $>10^7$ s^{-1} for all assemblies.

Gel electrophoresis studies of the damage products generated upon irradiation of these assemblies reveal that neither the guanine close to the Ru-complex intercalation site nor guanine bases surrounding the indole are damaged (data not shown). As with earlier experiments (vide supra), only damage to the 4-methylindole base is observed, and the level of damage is comparable in these assemblies. It is noteworthy that all of these experiments have been conducted at ruthenated duplex concentrations <25 μM, where no interduplex reactions are detected.[53]

Figure 7 shows the transient absorption traces generated with Ru−DNA sequences **5**−**8** recorded at 600 nm. The short-lived transient observed at this wavelength could be assigned (vide supra) to the 4-methylindole radical cation. Kinetic data for the recovery of the Ru(II) signal and the formation of the 4-methylindole radical are listed in Table 2. The signal at 600 nm is initially negative but crosses over the baseline within 1 μs to give a positive signal, corresponding to the formation of the 4-methylindole radical cation. The traces were fit to a monoexponential function indicating that the formation of the radical cation occurs with a rate constant of $k = 3 \times 10^7$ s^{-1}, indistinguishable from the time scale of the emission of $*[Ru(dppz)(phen)_2]^{2+}$ bound to DNA.

The decay of the radical can be observed on a longer time scale (100 μs). Fitting the decay of the 4-methylindole radical cation to a monoexponential function reveals a rate of 10^5 s^{-1} for all assemblies. Compared to the lifetime of the guanine radical, the lifetime of the 4-methylindole radical cation is, again, at least an order of magnitude shorter.

The recovery of Ru(II) was also examined by following the transients at 440 nm (data not shown). Monitoring at this wavelength allows us to probe the kinetics of the hole injection into DNA. These traces initially exhibit a negative spike due to bleaching of the Ru(II)−ligand MLCT band. Fitting a monoexponential function to these traces reveals a rate of at least 10^7 s^{-1}. On the basis of the weak signal observed in this regime, however, it is clear that faster time components must also exist.

Thus, the rates generated from the kinetic traces of the four sequences clearly show no distance dependence in the formation

of the indole radical cation. For the formation of the 4-methylindole radical cation monitored at 600 nm, the same rate $k > 10^7\ s^{-1}$ for all four assemblies was determined (Table 2). Thus, the rate of radical cation formation is coincident with quenching of the ruthenium excited state to form the Ru(III) oxidant. Charge transport through the DNA, remarkably, with as many as 8 intervening Ts, is not rate-limiting. What may instead be rate-limiting here is diffusion of the quencher.

These data also show that the yield of generated 4-methylindole radical cation is not influenced by the length of the intervening bridge. Figure 7b shows the transient absorption traces recorded at 600 nm on a 100 μs time scale. The intensity of the signal appearing within approximately 5 μs is the same for all four sequences. Therefore, no distance dependence in the yield of radical could be observed.

Mechanistic Considerations. These data require consideration in the context of current models for DNA charge transport. The original model of G-hopping and AT-tunneling, as proposed by Giese and Jortner,[23,24] clearly is not sufficient to account for these data; assuming a decay factor, β, equal to 0.6 $Å^{-1}$, the rate of tunneling through 8 AT base pairs would be vanishingly small. We had, however, already shown, through measurements of the yield of long-range oxidative damage to GG doublets, that hopping through domains containing AT-tracts was necessary.[18] The measurements here of rates of radical cation formation confirm that conclusion.

More recently, Giese and co-workers have carried out experiments in which oxidative damage yields were measured that pointed to a mixture of tunneling and hopping regimes; consistent with theoretical proposals of Jortner, tunneling through 2−3 AT base steps was expected with hopping over longer AT regions.[22] Our data, strictly taken, also do not provide direct support for this proposal. Such a proposal would predict over short distances, in particular for assembly **5**, that the rate of charge transport would be 10^2-10^3 times faster compared to those of assemblies **6**−**8** with longer distances of charge transport. One could argue that our results are compatible with this proposal because our measured rates of radical cation formation can only reflect lower limits on charge transport. Nonetheless, one might have expected that the yield of oxidation would be significantly higher for assembly **5**.

Our measured rates of radical formation over a charge transport distance of 37 Å also differ from indirect spectroscopic measurements of hole transport by Lewis and co-workers.[59] Those studies suggested that base/base transport would be significantly slower over this distance range. Perhaps generally, the faster rates we observe can be explained in part on the basis of effective coupling of the ruthenium intercalator within the base pair stack. Lewis and co-workers have utilized stilbenes as photooxidants,[4] and in the case of Giese's studies, the radical is generated first on the sugar.[3] Neither is expected to be as well coupled into the base pair stack as an intercalator.

Another issue to consider is the pathway for such charge transport. Energetically, thymine bridges are significantly disfavored compared to adenine bridges. It has been proposed, however, that intrastrand thymine−thymine coupling is effective and that interstrand and intrastrand adenine−adenine couplings are comparable.[60] Our experimental data on base−base electron transfer indicated, however, a penalty in rate of 3 orders of magnitude in interstrand versus intrastrand transfer. Intra- and interstrand rates may converge, however, over longer molecular distances.

The studies described here are in fact most easily reconciled with these earlier ultrafast measurements of DNA charge transport.[9,10] We have proposed that charge transport through DNA occurs primarily through hopping among domains defined by DNA sequence and dynamics.[9,10,16,18] Schuster has described DNA charge transport in terms of an analogous, although distinct, polaron domain hopping model but without proposals for the kinetics.[17,61] Base−base hopping, gated by base pair dynamics, or tunneling has been found in ultrafast measurements to occur with rates of $10^{10}\ s^{-1}$.[9,10] Such hopping and tunneling times would account well for the data obtained here.

Currently, however, the flash-quench method allows us only to establish the lower limit in the rate of radical formation through DNA-mediated charge transport at a distance of 37 Å, and this rate appears to be simultaneous with the rate of intercalated oxidant formed upon excited-state quenching by the diffusing quencher. Just as classic attempts to map out the inverted Marcus region for electron transfer in σ-systems were first thwarted by the diffusion limit,[62] so too are current studies of rates of DNA charge transport over long molecular distances.

Acknowledgment. We are grateful to the NIH for financial support (GM49216). M.P. also thanks the Deutscher Akademischer Austauschdienst for a postdoctoral fellowship. In addition, we thank Prof. E. D. A. Stemp and Prof. S. Rajski for valuable discussions and S. Delaney for experimental assistance.

JA0202210

(59) Lewis, F. D.; Liu, X.; Liu, J.; Miller, S. E.; Hayes, R. T.; Wasielewski, M. R. *Nature* **2000**, *406*, 51.

(60) (a) Voityuk, A. A.; Rosch, N.; Bixon, M.; Jortner, J. *J. Phys. Chem. B.* **2000**, *104*, 9740. (b) Voityuk, A. A.; Bixon, M.; Rosch, N.; Jortner, J. *J. Chem. Phys.* **2001**, *114*, 5614.

(61) Barnett, R. N.; Cleveland, C. L.; Joy, A.; Landman, U.; Schuster, G. B. *Science* **2001**, *294*, 567.

(62) (a) Marcus, R. A. *Annu. Rev. Phys. Chem.* **1964**, *15*, 155. (b) Marcus, R. A.; Sutin, N. *Biochim. Biophys. Acta*. **1985**, *811*, 265.